Electronic Supplementary Material (ESI) for RSC Advances.

Controllable synthesis of high quality monolayer WS_2 on SiO_2/Si substrate by chemical vapor deposition

Qi Fu,[a] Wenhui Wang,[a] Lei Yang,[a] Jian Huang,[a] Jingyu Zhang,[c] Bin Xiang*[a,b]

[a]Department of Materials Science & Engineering, CAS key Lab of Materials for Energy Conversion, University of Science and Technology of China, Hefei, Anhui, 230026, China.

* E-mail: binxiang@ustc.edu.cn

[b]Synergetic Innovation Center of Quantum Information & Quantum Physics, University of Science and Technology of China, Hefei, Anhui 230026, China

[c]Molecular Foundry, Lawrence Berkeley National Laboratory, 1 Cyclotron Rd, Berkeley, CA 94720, USA

The Schematic representation of our experimental setup and details of temperature ramp.

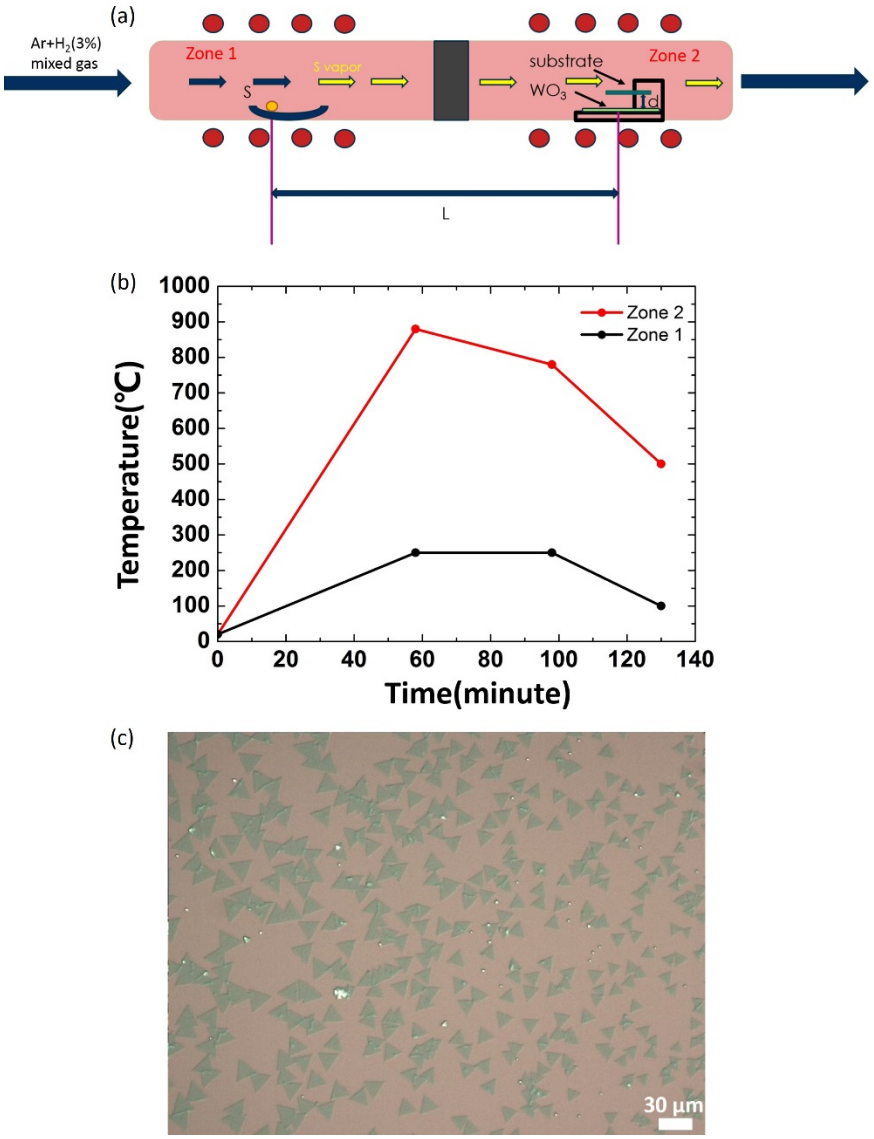

Figure S1. (a) The Schematic representation of experimental setup. (b) Temperature ramp of the fine growth condition. (c) Optical image of the large-area as-grown monolayer WS_2 triangular domains.

Details of multipeak Lorentzian fitting in Raman spectrum.

Peaks	$2LA - 2E_{2g}^{2}$	$E_{2g}^{1}(M)$	$2LA(M)$	$E_{2g}^{1}(\Gamma)$
Position (cm^{-1})	324.3 (2.79)	348.9 (1.83)	351.5 (0.32)	354.4 (0.82)
FWHM(cm^{-1})	16.30 (2.79)	10.52 (3.20)	12.21 (0.96)	6.51 (2.81)
Intensity (normalized)	0.14	0.63	0.91	0.63

Table 1. Peaks position, FWHM and intensity of resolved Raman spectrum in Figure 2a. The value in the bracket represents fitting error of peak position and FWHM.

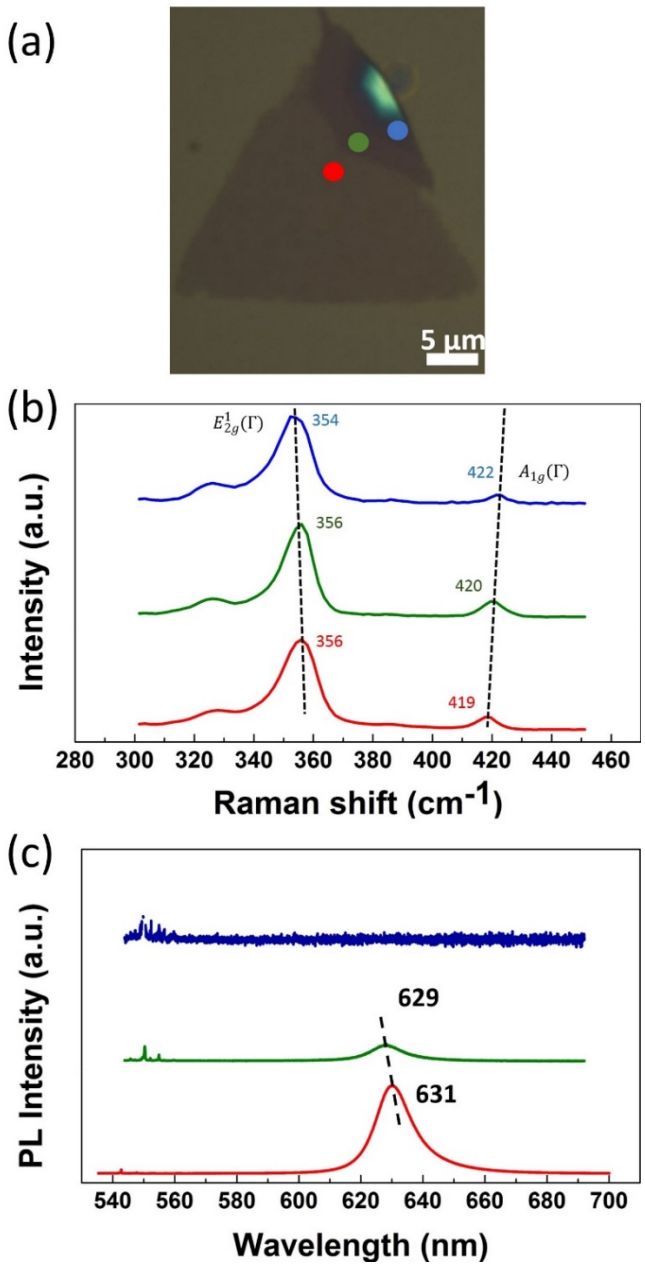

Figure S2. (a) One WS_2 triangle with different thickness at different sites. (b) The frequency change of $E^1_{2g}(\Gamma)$ and $A_{1g}(\Gamma)$ peaks at three different sites marked in (a), the spots in (a) and profiles in (b) corresponds in color. (c) PL location and intensity differ at different sites marked in (a).

Optical image of an substrate area before and after heated to 950 °C.

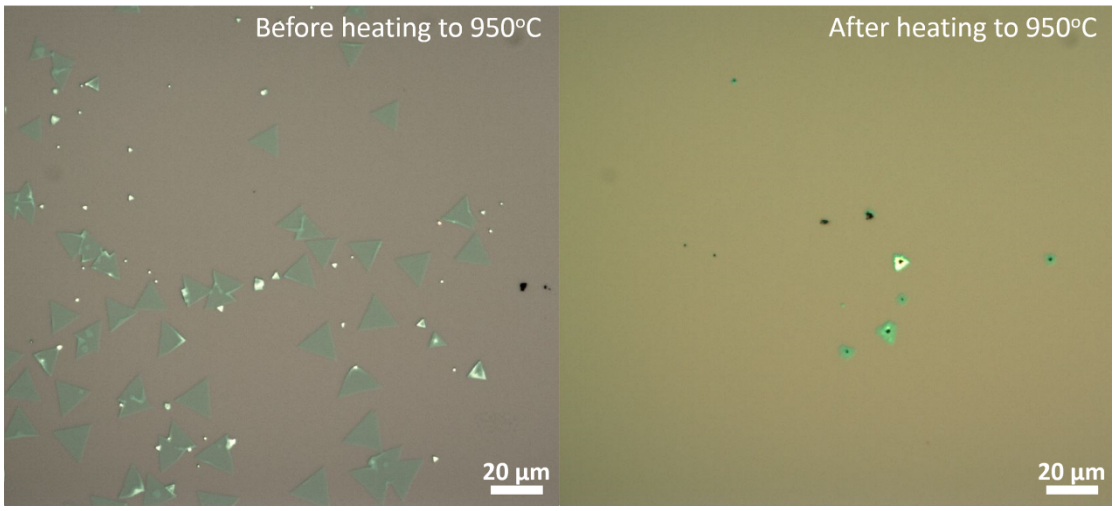

Figure S3. The left part of the image exhibits as-grown WS_2 triangular domains, and the substrate was heated to 950 °C, the right part of the image exhibits the same area after the heating process.

Optical image of WS_2 triangular grown under gas flow rate of 20, 50 and 80 sccm. Some other parameters: 0.015 g of sulfur powder and 0.5 g of WO_3 powder were loaded, the sulfur powder was heated to 250 ^oC and the WO_3 powder was heated to 880 ^oC at 15 ^oC/min.

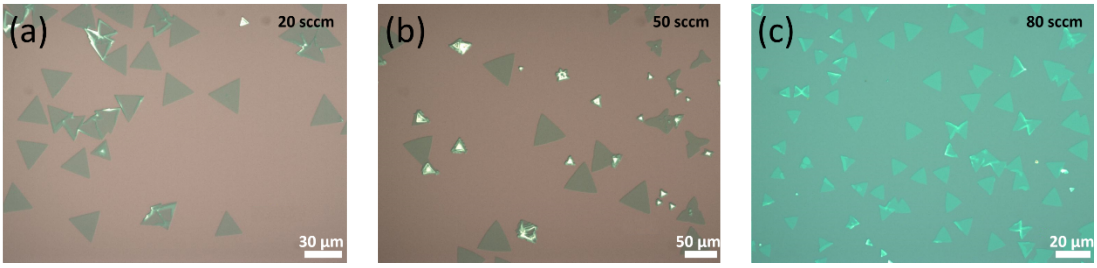

Figure S4. Optical image of WS_2 triangular grown under (a) 20 sccm, (b) 50 sccm and (c) 80 sccm.

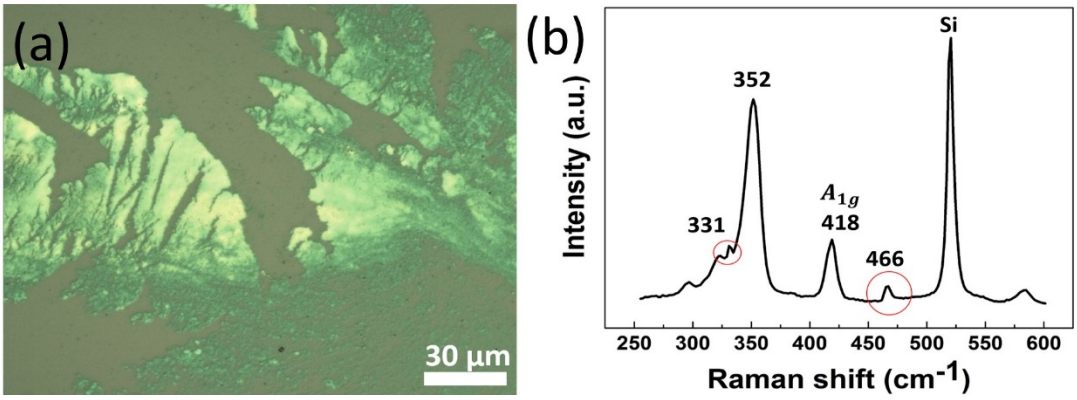

Figure S5. (a) Optical image of WS_2 flake grown under sulfur-lack condition. (b) Raman spectra of deposition shown in (a). The two peaks as marked by red circle indicate the existence of the impurity deposition.

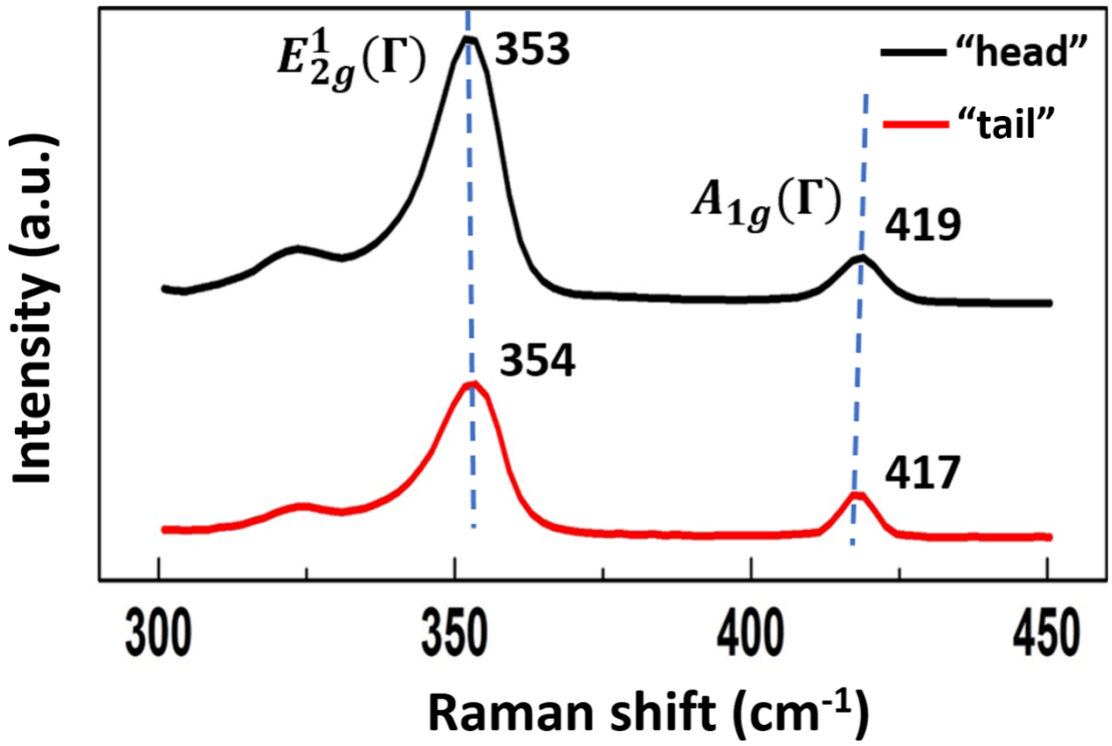

Figure S6. Raman spectra of the "head" and the "tail" of the comet-like WS_2 domains grown under 100 sccm.

We have done a series of WS_2 growth experiments by only varying the growth time in order to control the amount of precursors involved in the growth reactions. As shown in Figure S7, there are incomplete-shape triangular domains observed when growth time is 1 min. With an increase of growth time, there are more precursors involved in the growth reactions. As a result, we observed complete triangular domain growth with a size of ~ 25 μm. Our results indicate that growth time is another important parameter to control the morphologies of the as-grown WS_2 domains by limiting the amount of precursors involved in the growth reactions.

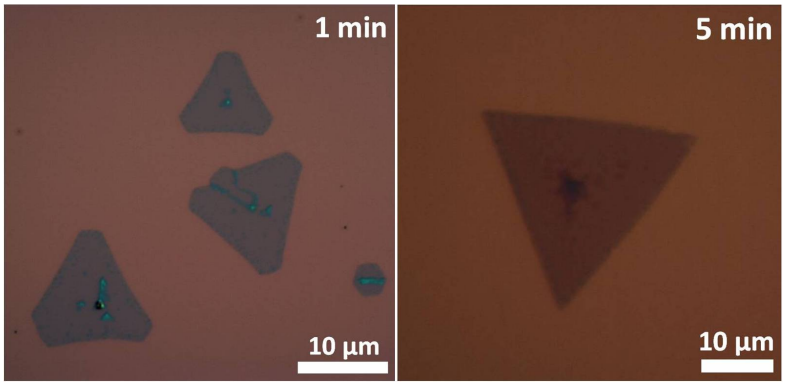

Figure S7. WS_2 triangular domain growth at different growth time. In the meanwhile we kept other growth parameters as the same.